LETTER

doi:10.1038/nature14350

A Mercury-like component of early Earth yields uranium in the core and high mantle ^{142}Nd

Anke Wohlers[1] & Bernard J. Wood[1]

Recent ^{142}Nd isotope data indicate that the silicate Earth (its crust plus the mantle) has a samarium to neodymium elemental ratio (Sm/Nd) that is greater than that of the supposed chondritic building blocks of the planet. This elevated Sm/Nd has been ascribed either to a 'hidden' reservoir in the Earth[1,2] or to loss of an early-formed terrestrial crust by impact ablation[3]. Since removal of crust by ablation would also remove the heat-producing elements—potassium, uranium and thorium—such removal would make it extremely difficult to balance terrestrial heat production with the observed heat flow[3]. In the 'hidden' reservoir alternative, a complementary low-Sm/Nd layer is usually considered to reside unobserved in the silicate lower mantle. We have previously shown, however, that the core is a likely reservoir for some lithophile elements such as niobium[4]. We therefore address the question of whether core formation could have fractionated Nd from Sm and also acted as a sink for heat-producing elements. We show here that addition of a reduced Mercury-like body (or, alternatively, an enstatite-chondrite-like body) rich in sulfur to the early Earth would generate a superchondritic Sm/Nd in the mantle and an ^{142}Nd/^{144}Nd anomaly of approximately +14 parts per million relative to chondrite. In addition, the sulfur-rich core would partition uranium strongly and thorium slightly, supplying a substantial part of the 'missing' heat source for the geodynamo.

Terrestrial rocks were recently found to have higher ratios of radiogenic ^{142}Nd to nonradiogenic ^{144}Nd than do the chondritic meteorites generally supposed to be representative of the material from which Earth accreted[1,2]. ^{142}Nd was produced during the early history of the Solar System from decay of the extinct radionuclide ^{146}Sm (half-life, $t_{1/2}$ = 68 million years[5] and the presence of a positive ^{142}Nd anomaly of ~20 parts per million (p.p.m.) calculated as $10^6\left[\left(\frac{^{142}Nd}{^{144}Nd}\right)_{Earth} - \left(\frac{^{142}Nd}{^{144}Nd}\right)_{chondrite}\right] / \left(\frac{^{142}Nd}{^{144}Nd}\right)_{Earth}$ or of ~9 p.p.m.[6] in the silicate Earth would require an Sm/Nd ratio higher than chondritic[1,2]. This high Sm/Nd ratio was established early in Earth's history while ^{146}Sm was still 'alive' (that is, undergoing radioactive decay).

A plausible mechanism for generating high Sm/Nd in Earth's mantle is partial melting and melt extraction to form a crust. Because Nd is less compatible in mantle silicates than Sm[7], partial melts have relatively low Sm/Nd and the solid residue has high Sm/Nd. A low-Sm/Nd crust could be completely removed from the mantle system by subduction to an inaccessible region of the deep mantle[1] or removed from Earth by impact ablation[3]. The problem with the former hypothesis is the lack of evidence for a hidden silicate reservoir, while the latter hypothesis suffers from the requirement that much of Earth's heat production, in the form of radioactive uranium (U), thorium (Th) and potassium (K) would be removed together with the low-Sm/Nd crust. Assuming chondritic abundances of U and Th and a K/U ratio of ~12,000 for the silicate Earth[8], the heat production in the Earth is only about 0.6 times the current heat loss[9]. Reducing the heat sources further by ablation loss would make it even more difficult to reconcile heat production with heat loss.

An additional question in the context of heat production is that of the energy source for the Earth's magnetic field[10]. Arising from convection in the core, Earth has had a magnetic field for at least 3.5 billion years. The crystallization of the inner core is an important source of energy for the geodynamo[11] but most attempts to construct histories of core cooling indicate that the inner core cannot be much older than 1–1.5 billion years[10,11] unless a source of radioactive heating is present. Numerous studies have focused on ^{40}K as a potential core heat source, because K, in common with all moderately volatile elements[8], is depleted in the silicate Earth relative to the chondritic abundance.

Furthermore, high-pressure experiments[12,13] indicate that K enters sulfide under oxidizing conditions and sulfur (S) is believed to be a major component of the core's complement of approximately 10% of elements of low atomic number[14]. It appears, however that the maximum possible K content of the core is insufficient to generate more than a small fraction of the 2–5 TW required to generate reasonable core thermal histories[11,13]. The alternative explanation—that U and/or Th provide the energy for core convection—has some support from early experiments on sulphide–silicate partitioning[15] but more recent results indicate very little partitioning of U into S-bearing metals even under extreme conditions[16].

We approached the problem of U, Th, Nd and Sm in Earth's mantle and core from the standpoint of recent work on partitioning between sulfide melts and silicate melts[17]. Kiseeva and Wood[17] found that the sulfide–silicate partition coefficient for any element i, defined as $D_i = [i]_{sulf}/[i]_{sil}$, is dependent on the FeO content of the silicate melt, such that for FeS-rich sulfides:

$$\log D_i = A - n\log[\mathrm{FeO}] \quad (1)$$

where A is a constant and n is a constant dependent on the valency of element i. Therefore, under strongly reducing conditions, where the FeO content of the silicate melt is very low (<1% for example) one would expect D_i values to be much higher than under the conditions of MORB crystallization where the FeO content of the melt is about 8%–10%. This hypothesis is consistent with the data of Murrell and Burnett[15], who observed strong partitioning of U into sulfide liquid at low oxygen fugacity f_{O2}. Given terrestrial accretion models calling for prolonged periods of growth under reduced conditions[18,19], the demonstration that Mercury is a highly reduced S-rich planet with a liquid core[20,21] and the association of the rare earth elements (REEs), U and Th with sulfides in enstatite chondrite meteorites[22], we investigated partitioning of U, Th, Sm, Nd and several other lithophile elements into liquid iron sulfide under reducing conditions.

Experiments were performed at 1.5 GPa and temperatures between 1,400 °C and 1,650 °C using starting materials that were approximately 50:50 mixtures of silicate and FeS doped with a range of lithophile trace elements including U, Th, La, Nd, Sm, Eu, Yb, Ce, and Zr (see Methods). The silicate was a basalt-like composition in the system CaO–MgO–Al_2O_3–SiO_2 with variable FeO. Analysis

[1]Department of Earth Sciences, University of Oxford, South Parks Road, Oxford OX1 3AN, UK.

was by electron microprobe and laser ablation inductively coupled plasma mass spectrometry (LA-ICP-MS) (Methods). Table 1 presents a summary of sulfide–silicate partitioning results (see Extended Data Figs 1–3 and Extended Data Tables 1–4 for complete analyses).

Figure 1a shows data from a series of experiments performed at 1,400 °C. As can be seen, the partition coefficients of U, Nd and Sm are strong functions of the FeO content of the silicate melt, increasing dramatically, as predicted, as the FeO content decreases below 1 wt%. The negative slope of logD_i as f(log[FeO_{sil}]) reverses at high FeO_{sil}, however, because the sulfide dissolves progressively more oxygen as the FeO content of silicate increases and these three lithophile elements (Fig. 1a) follow oxygen into the sulfide. We found similar behaviour in two more series of experiments at higher temperature (Table 1 and Extended Data Fig. 1). Other lithophile elements, notably Ti, Nb and Ta (B.J.W., unpublished data) behave similarly. Importantly, we find $D_U > D_{Nd} > D_{Sm}$ for partitioning into sulfide in all experiments. At very low FeO contents all D_i become >1 (Fig. 1a). Furthermore (Fig. 1b) D_{Nd} is always appreciably greater than D_{Sm}, with D_{Nd}/D_{Sm} approaching 1.5 in some cases.

The implications of Fig. 1 are that segregation of sulfide (or S-rich metal) from reduced FeO-poor silicate will lead to enrichment of the metallic phase in U and in Nd relative to Sm when compared to the silicate. Addition of such material to the core and mantle respectively of a growing planet would provide a core heat source and a mantle with superchondritic Sm/Nd, Yb/Sm and Yb/La. Although potentially detectable in terms of a mantle ^{142}Nd anomaly, the fractionation of heavy from light REEs (Table 1) in the primitive mantle of the body (the bulk silicate Earth in this case) would have little effect on its overall REE pattern (Extended Data Fig. 3). Similarly, there would be no observable Eu anomaly despite the fact that Eu is probably in the 2^+ oxidation state (unlike the other 3^+ lanthanides) under these conditions (Extended Data Fig. 3). If such a body represented Earth early in its history then the mantle would have a positive ^{142}Nd anomaly relative to chondrite (as observed) and much of the energy deficit identified for core convection[10] would be supplied by U (and Th). We find that D_{Th}/D_U is about 0.1, indicating that U would be accompanied by Th in the S-rich core. Addition of more-oxidized material later in accretion would lead to the higher current FeO content of the mantle (8.1%)[8], but could not erase the superchondritic Sm/Nd ratio of the mantle and U content of the core unless there were complete core–mantle re-equilibration.

Figure 2 illustrates the impact of adding a highly reduced body rich in sulfide to the growing Earth. The Th/U ratio of the silicate Earth would be higher than chondritic (3.8–3.9[8,23]), which provides an important constraint on how much U can be present in Earth's core. Based on the Pb-isotopic compositions of Archean galenas[24] and of 3.5-billion-year-old komatiites[25] the Th/U ratio of the Archean mantle has been estimated to be ≥4.3. Tatsumoto[26] argued, on the basis of the Pb isotopic compositions of basalts, for an early differentiation of the mantle, which resulted in a Th/U of 4.2–4.5 in the mantle source regions. Since that time the Th/U ratio of the mantle has decreased, probably owing to preferential recycling of the more soluble U[27].

Figure 2 shows four models of U content of the core and the ^{142}Nd anomaly of the mantle (relative to the bulk Earth), based on our partitioning data. We choose a reduced body of 0.15 mass fraction sulphide, corresponding to the S content of primitive CI chondrites[8] and use values of D_{Sm} (Sm_{sulf}/Sm_{sil}) that are close to the observed maximum of 0.8–2.2, noting that D_{Sm} values increase with decreasing temperature and that segregation of sulfide from a crystal-melt mush instead of melt alone would increase them further because of the incompatibility of Sm, Nd and U in crystals. As can be seen (Fig. 2a), adding 20% of such a body to Earth would lead to 4–5 parts per billion (p.p.b.) of U in the core, a Th/U of the silicate Earth of 4.17 and a ^{142}Nd anomaly in the mantle relative to the bulk Earth

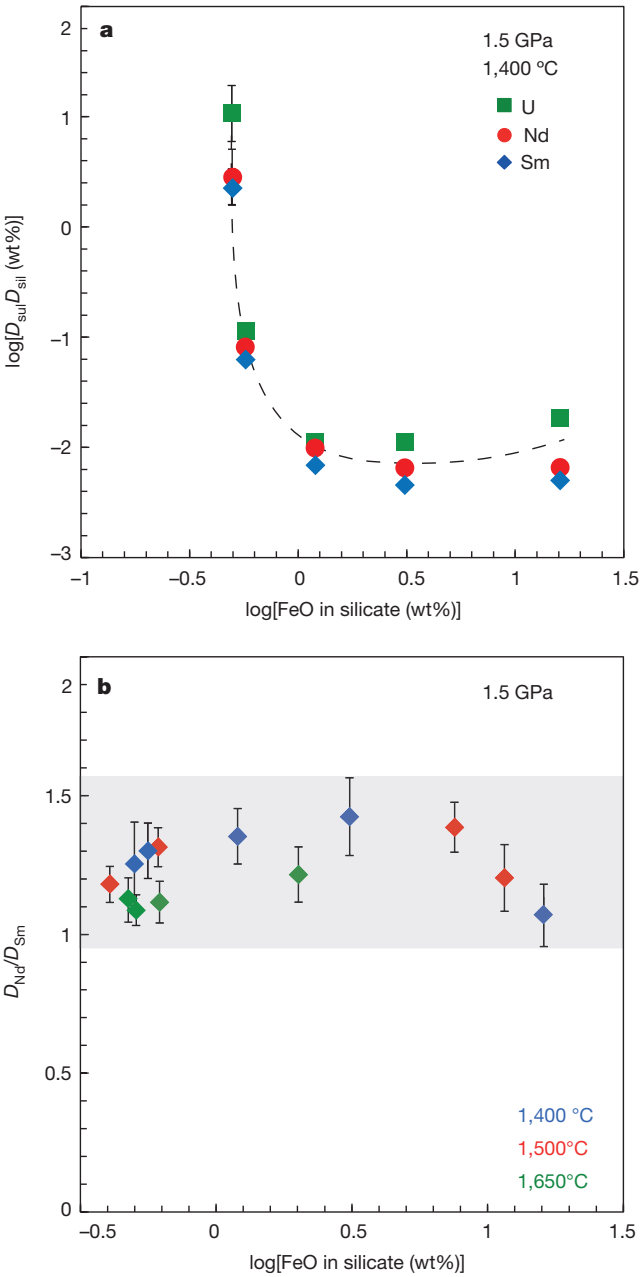

Figure 1 | Sulphide–silicate partitioning data. a, Partition coefficients $D_i = [i]_{sulf}/[i]_{sil}$ for U, Nd and Sm at 1.5 GPa and 1,400 °C plotted versus the log of the FeO content of the silicate melt in weight per cent. **b**, The ratio of D_{Nd}/D_{Sm} plotted versus log[FeO]. Error bars in both cases are ±2 s.e. and, if absent, are smaller than symbol size.

of ~7 p.p.m. Increasing the reduced body mass to 45% (Fig. 2b) leads to about 8 p.p.b. U in the core, a Th/U of the silicate Earth of 4.5 and a mantle ^{142}Nd anomaly of 13.9 p.p.m. relative to the bulk Earth.

We performed a sensitivity analysis (Extended Data Fig. 2) and find that, if the Th/U of the silicate Earth is ≤4.5, the maximum U content of the core is 8 p.p.b. with a Th content of ~8 p.p.b. These figures increase to ~10 p.p.b. if the Th/U of the silicate Earth is ≤4.7. The ^{142}Nd anomaly is 13.9 p.p.m. in the former case and ~17 p.p.m. in the latter. The estimated U and Th contents of the core would lead to 2–2.4 TW, sufficient to power the geodynamo[11] even without the potential 0.4–0.8 TW from ^{40}K decay[13]. We can reduce the size of the reduced body by increasing its S content (Fig. 2c, d) and increase D_U/D_{Sm} but the overall effects on the core and mantle ^{142}Nd remain

Table 1 | Summary of sulfide–silicate partition coefficients

Run	Pressure, P (GPa)	Temperature, T (°C)	log[FeO_{sil}(wt%)]	D_{Sm}	D_{Nd}/D_{Sm}	D_U/D_{Sm}	D_{Th}/D_U	D_{Eu}/D_{Sm}	D_{La}/D_{Sm}	D_{Yb}/D_{Sm}
421	1.5	1,400	0.50	0.005	1.42	2.47	0.036	5.85	1.38	0.16
σ				0.001	0.29	0.37	0.008	0.93	0.23	0.07
428	1.5	1,400	0.08	0.013	1.35	1.56	0.038	5.50	1.35	0.16
σ				0.001	0.19	0.17	0.005	1.06	0.20	0.02
427	1.5	1,400	−0.25	0.062	1.30	1.81	0.028	2.36	1.23	0.13
σ				0.006	0.19	0.24	0.004	0.40	0.22	0.02
426	1.5	1,400	−0.30	2.247	1.25	6.81	0.048	0.14	1.03	0.16
σ				0.333	0.30	1.43	0.010	0.05	0.15	0.09
429	1.5	1,400	1.21	0.005	1.04	3.68	0.200	2.04	1.10	0.67
σ				0.0001	0.12	0.89	0.041	0.42	0.47	0.19
461	1.5	1,650	0.30	0.023	1.22	1.92	0.058	4.09	1.18	0.21
σ				0.003	0.20	0.32	0.009	0.58	0.18	0.03
462	1.5	1,650	−0.21	0.154	1.12	3.58	0.046	1.13	0.92	0.27
σ				0.011	0.13	0.43	0.007	0.14	0.10	0.03
477	1.5	1,650	−0.29	0.629	1.10	9.26	0.044	0.37	0.83	0.39
σ				0.038	0.11	0.73	0.043	0.38	0.80	0.39
464	1.5	1,650	−0.32	0.751	1.13	9.41	0.035	0.21	0.55	0.28
σ				0.073	0.16	1.18	0.020	0.16	0.44	0.16
1,414	1.5	1,500	−0.21	0.048	1.31	1.84	0.031	5.95	1.41	0.13
σ				0.004	0.14	0.34	0.009	0.80	0.16	0.02
1,415	1.5	1,500	−0.39	0.454	1.18	6.99	0.040	0.88	1.04	0.21
σ				0.028	0.13	0.66	0.005	0.11	0.14	0.05
1,416	1.5	1,500	0.88	0.006	1.39	2.70	0.067	4.92	1.52	0.23
σ				0.0005	0.18	0.25	0.007	0.56	0.19	0.02
1,417	1.5	1,500	1.06	0.007	1.20	3.11	0.150	2.71	1.19	0.50
σ				0.001	0.24	0.52	0.042	0.48	0.21	0.30

Partition coefficients in weight ratio. σ is calculated from error propagation.

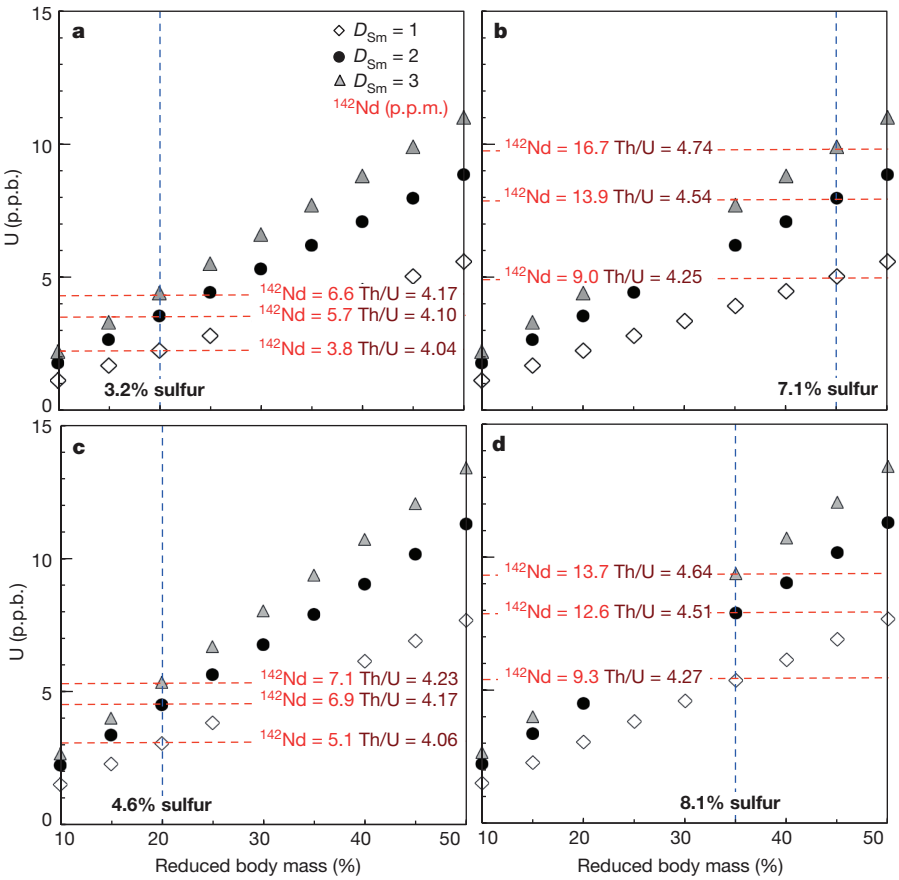

Figure 2 | Core content of U (p.p.b.) and mantle ^{142}Nd anomaly (p.p.m.). a, Calculated effect of adding to the growing Earth a reduced body of 20% of Earth's mass containing 0.15 mass fraction sulfide. The sulfide is added to the core and the silicate to the mantle. Sulphide–silicate D_U/D_{Sm} is fixed at 2, D_{Nd}/D_{Sm} at 1.4 and D_{Th}/D_U at 0.1 (Table 1). **b**, Same as **a** except the mass of reduced body is 45% of the Earth's mass. **c** and **d**, As for **a** and **b** except the reduced body contains 0.22 mass fraction sulfide. The reduced body and remainder of Earth each contain 14 p.p.b. U and 53.5 p.p.b. Th, consistent with chondritic abundances. Sulfide extraction was assumed to take place at the origin of the Solar System.

close to those summarized above if the Th/U of the bulk silicate Earth is constrained to be ≤4.5 or ≤4.7.

We note that the scenarios shown in Fig. 2 refer to a terrestrial core containing between 3.2 wt% S and 8.1 wt% S. The concentration of cosmochemically abundant volatile S in the core is unknown, but recent suggestions range from a cosmochemical estimate of 1.7 wt% (ref. 14) to ~6 wt% (ref. 28) from liquid-metal density measurements and 14.7 wt% (ref. 29) from high-temperature, high-pressure equation-of-state measurements. The range shown in Fig. 2 is, therefore appropriate for the current state of knowledge.

We conclude that a period of growth of the accreting Earth under reduced, S-rich conditions would generate a measureable (~+14 p.p.m.) ^{142}Nd anomaly in the silicate Earth, in agreement with observations. This would also add sufficient U and Th to the core to generate 2–2.4 TW of the energy required to drive the geodynamo.

Online Content Methods, along with any additional Extended Data display items and Source Data, are available in the online version of the paper; references unique to these sections appear only in the online paper.

Received 17 December 2014; accepted 20 February 2015.

1. Boyet, M. & Carlson, R. W. ^{142}Nd evidence for early (>4.53 Ga) global differentiation of the silicate Earth. *Science* **309,** 576–581 (2005).
2. Boyet, M. & Carlson, R. W. A new geochemical model for the Earth's mantle inferred from (SM)-S-146-Nd-142 systematics. *Earth Planet. Sci. Lett.* **250,** 254–268 (2006).
3. Campbell, I. H. & O'Neill, H. S. C. Evidence against a chondritic Earth. *Nature* **483,** 553–558 (2012).
4. Wade, J. & Wood, B. J. The Earth's 'missing' niobium may be in the core. *Nature* **409,** 75–78 (2001).
5. Kinoshita, N. *et al.* A shorter Sm-146 half-life measured and implications for Sm-146-Nd-142 chronology in the Solar System. *Science* **335,** 1614–1617 (2012).
6. Sprung, P., Kleine, T. & Scherer, E. E. Isotopic evidence for chondritic Lu/Hf and Sm/Nd of the Moon. *Earth Planet. Sci. Lett.* **380,** 77–87 (2013).
7. Blundy, J. D. & Wood, B. J. Prediction of crystal–melt partition coefficients from elastic moduli. *Nature* **372,** 452–454 (1994).
8. Palme, H. & O'Neill, H. S. C. in *The Mantle and Core Vol. 2 Treatise on Geochemistry* (ed. Carlson, R. W.) 1–38 (Elsevier, 2003).
9. Stein, C. A. in *Global Earth Physics: A Handbook of Physical Constants* (ed. Ahrens, T. J.) 144–158 (American Geophysical Union, 1995).
10. Labrosse, S., Poirier, J. P. & Le Mouel, J. L. The age of the inner core. *Earth Planet. Sci. Lett.* **190,** 111–123 (2001).
11. Nimmo, F., Price, G. D., Brodholt, J. & Gubbins, D. The influence of potassium on core and geodynamo evolution. *Geophys. J. Int.* **156,** 363–376 (2004).
12. Gessmann, C. K. & Wood, B. J. Potassium in the Earth's core? *Earth Planet. Sci. Lett.* **200,** 63–78 (2002).
13. Murthy, V. M., van Westrenen, W. & Fei, Y. W. Experimental evidence that potassium is a substantial radioactive heat source in planetary cores. *Nature* **423,** 163–165 (2003).
14. Dreibus, G. & Palme, H. Cosmochemical constraints on the sulfur content in the Earth's core. *Geochim. Cosmochim. Acta* **60,** 1125–1130 (1996).
15. Murrell, M. T. Partitioning of K, U, and Th between sulfide and silicate liquids—implications for radioactive heating of planetary cores. *J. Geophys. Res.* **91,** 8126–8136 (1986).
16. Wheeler, K. T., Walker, D., Fei, Y. W., Minarik, W. G. & McDonough, W. F. Experimental partitioning of uranium between liquid iron sulfide and liquid silicate: implications for radioactivity in the Earth's core. *Geochim. Cosmochim. Acta* **70,** 1537–1547 (2006).
17. Kiseeva, E. S. & Wood, B. J. A simple model for chalcophile element partitioning between sulphide and silicate liquids with geochemical applications. *Earth Planet. Sci. Lett.* **383,** 68–81 (2013).
18. Wade, J. & Wood, B. J. Core formation and the oxidation state of the Earth. *Earth Planet. Sci. Lett.* **236,** 78–95 (2005).
19. Rubie, D. C. *et al.* Heterogeneous accretion, composition and core-mantle differentiation of the Earth. *Earth Planet. Sci. Lett.* **301,** 31–42 (2011).
20. Nittler, L. R. *et al.* The major-element composition of Mercury's surface from MESSENGER X-ray spectrometry. *Science* **333,** 1847–1850 (2011).
21. Smith, D. E. *et al.* Gravity field and internal structure of Mercury from MESSENGER. *Science* **336,** 214–217 (2012).
22. Gannoun, A., Boyet, M., El Goresy, A. & Devouard, B. REE and actinide microdistribution in Sahara 97072 and ALHA77295 EH3 chondrites: a combined cosmochemical and petrologic investigation. *Geochim. Cosmochim. Acta* **75,** 3269–3289 (2011).
23. Blichert-Toft, J., Zanda, B., Ebel, D. S. & Albarede, F. The Solar System primordial lead. *Earth Planet. Sci. Lett.* **300,** 152–163 (2010).
24. Hofmann, A. W. Reviving the layered mantle: plan D. *American Geophysical Union Fall Meeting* Abstract V43E–05 http://abstractsearch.agu.org/meetings/2011/FM/V43E-05.html (2011).
25. Allègre, C. J., Dupre, B. & Lewin, E. Thorium uranium ratio of the Earth. *Chem. Geol.* **56,** 219–227 (1986).
26. Tatsumoto, M. Isotopic composition of lead in oceanic basalt and its implication to mantle evolution. *Earth Planet. Sci. Lett.* **38,** 63–87 (1978).
27. Elliott, T., Zindler, A. & Bourdon, B. Exploring the kappa conundrum: the role of recycling in the lead isotope evolution of the mantle. *Earth Planet. Sci. Lett.* **169,** 129–145 (1999).
28. Morard, G. *et al.* The Earth's core composition from high pressure density measurements of liquid iron alloys. *Earth Planet. Sci. Lett.* **373,** 169–178 (2013).
29. Seagle, C. T., Campbell, A. J., Heinz, D. L., Shen, G. Y. & Prakapenka, V. B. Thermal equation of state of Fe3S and implications for sulfur in Earth's core. *J. Geophys. Res.* **111,** B06209 (2006).

Acknowledgements We acknowledge support from the European Research Council grant number 267764. We thank J. Wade for his advice and comments. A. Hofmann and T. Elliott provided advice and suggestions about Th/U of silicate Earth.

Author Contributions Both authors performed experiments and microanalysis, with about two-thirds done by A.W. Both authors contributed to writing the manuscript, with about two-thirds done by B.J.W.

Author Information Reprints and permissions information is available at www.nature.com/reprints. The authors declare no competing financial interests. Readers are welcome to comment on the online version of the paper. Correspondence and requests for materials should be addressed to A.W. (anke.wohlers@earth.ox.ac.uk) or B.J.W. (berniew@earth.ox.ac.uk).

METHODS

Experimental methods. Starting materials for high-pressure experiments consisted of mixtures of ~50 wt% (Fe,Ni)S and ~50% of a synthetic silicate approximating the 1.5 GPa eutectic composition in the anorthite–diopside–forsterite system[30]. The sulfide component was analytical-grade FeS doped with 1%–3% NiS. Trace elements were added as a mix consisting of Zr, La, Ce, Nd, Sm, Eu, Yb, Th and U as oxides. After adding the trace-element mix such that each element was present at 1,000–2,000 p.p.m., the silicate and sulfide starting materials were mixed in 50:50 proportions and ground under acetone for 20 min, then dried at 110 °C before the experiment. Starting compositions were loaded into 3 mm outer diameter and 1 mm inner diameter graphite capsules.

Experiments were conducted in a half-inch-diameter piston-cylinder apparatus using external cylinders either of $BaCO_3$-silica glass (at 1,500 °C and 1,650 °C) or CaF_2 (at 1,400 °C) and an 8 mm outer diameter graphite furnace with a 1-mm-thick wall. The unsealed capsule was separated from the graphite furnace by an interior MgO sleeve, with a 0.5-mm-thick alumina disk on top to prevent puncture by the thermocouple. Temperatures were controlled and monitored using a tungsten–rhenium thermocouple (W5%Re/W26%Re), and the temperature was maintained within ±1 °C. Experimental conditions were 1,400 °C, 1,500 °C and 1,650 °C at 1.5 GPa and with experiment durations between 1 h and 4.5 h. These times are sufficient to approach equilibrium in small graphite capsules[17]. Experiments were quenched by turning off the power supply. After quenching, the capsule was extracted from the furnace, mounted in acrylic and polished for further analyses with electron microprobe and LA-ICP-MS. All experimental charges contained sulfide blebs embedded in a silicate glass matrix.

Microanalysis. Samples were analysed on the JEOL 8600 electron microprobe in the Archaeology Department at the University of Oxford. Wavelength dispersive analyses of the major-element compositions of silicate glasses and sulfides were performed at 15 kV with a beam current of 20 nA and a 10 μm defocused beam (Extended Data Tables 1 and 2). At least 20 analyses were taken of the silicate and sulfide in each experiment. Count times for major elements (Si, Al, Ca, Mg, Fe in silicate, Fe in sulfide) were 30 s on the peak and 15 s background. Minor elements (S, Ni, O) were analysed for 60 s peak and 30 s background. We have previously noted Ni loss from similar experiments[17] and the principal reason for adding Ni was to provide an additional check on LA-ICP-MS analyses of the trace elements of interest (see below). A range of natural and synthetic standards was used for calibration. Standards for silicate were wollastonite (Si, Ca), jadeite (Al), periclase (Mg) and haematite (Fe). Standards for sulfides were Ni metal (Ni), galena (S) and haematite (Fe, O). Oxygen in the sulfides was determined using the Kα peak and LDE crystal.

We determined U and Sm contents of three product sulfides as a further check on the LA-ICP-MS analyses. In this case we measured the Mα peak for U and the Lα peak for Sm using standards of UO_2 and $SmPO_4$ respectively and a PET crystal. Operating conditions were 15 kV, 40 nA and a 10 μm beam. The count time for U was 120 s on peak and 60 s background. Sm was analysed for 150 s on the peak and 75 s background.

Trace elements in silicates and sulfides were measured by LA-ICP-MS employing a NexION 300 quadropole mass spectrometer coupled to a New Wave Research UP213 Nd:YAG laser at the University of Oxford. A laser repetition rate of 10 Hz and spot size of 25–50 μm were used for silicate glasses and sulfides (Extended Data Tables 3 and 4) with an energy density of ~12 J cm^{-2}. Operating in time-resolved mode, we employed 20 s of background acquisition, followed by ablation for 60 s. Between analyses we employed a 60–90 s 'wash-out' time. The following masses were counted: ^{24}Mg, ^{27}Al, ^{29}Si, ^{57}Fe, ^{60}Ni, ^{43}Ca, ^{90}Zr, ^{139}La, ^{140}Ce, ^{142}Nd, ^{152}Sm, ^{153}Eu, ^{174}Yb, ^{232}Th, ^{239}U. Our external standard was NIST610 glass and we typically collected three spectra of this at the beginning and end of each sequence of 10–15 unknowns. The BCR-2G standard was used as a secondary standard to check the accuracy of the calibration. Ablation yields were corrected by referencing to the known concentrations of Si and Ca (silicate glass) and Fe (sulfides), which had been determined by microprobe. Data reduction was performed off-line using the Glitter 4.4.3 software package (http://www.glitter-gemoc.com/) which enabled us to identify occasional sulfide inclusions in the silicate analyses. Since the Fe content of the NIST610 standard is only 460 p.p.m., the background is high and the matrices are very different, so cross-checks on the sulfide analyses were required. Therefore, we measured Ni with the electron microprobe and LA-ICP-MS. In agreement with Kiseeva and Wood[17], we observed no systematic offset between electron microprobe and LA-ICP-MS analyses for Ni (Extended Data Tables 2 and 4). Additionally, as discussed above, the U and Sm contents of the sulfides were measured by electron microprobe in three experimental charges (numbers 1415, 464, and 477). Between 20 and 43 electron probe analyses were performed on each sample. The highest U and Sm concentrations were measured in experiment 1415 with LA-ICP-MS (U = 2,958 p.p.m., Sm = 719 p.p.m.). Comparative measurements with electron probe yielded values of U = 3,280 ± 490 p.p.m. and Sm = 707 ± 110 p.p.m., (uncertainty is 2 s.e.) and therefore show excellent agreement. Two samples with lower U and Sm concentrations were also analysed. LA-ICP-MS measurements for experiment 464 yielded U = 952 p.p.m. and Sm = 327 p.p.m., while experiment 477 gave U = 927 p.p.m. and Sm = 300 p.p.m. Electron microprobe concentrations of U = 1,164 ± 224 p.p.m. and Sm = 319 ± 87 p.p.m. (experiment 464) and U = 991 ± 69 p.p.m. and Sm = 277 ± 38 p.p.m. (experiment 477) are also in excellent agreement with the LA-ICP-MS measurements. We conclude that our LA-ICP-MS results have no detectable systematic offset due to matrix effects or calibration errors.

30. Presnall, D. C. *et al.* Liquidus phase relations on the join diopside-forsterite-anorthite from 1 atm to 20 kbar: their bearing on the generation and crystallization of basaltic magma. *Contrib. Mineral. Petrol.* **66,** 203–220 (1978).
31. Salters, V. J. M. & Stracke, A. Composition of the depleted mantle. *Geochem. Geophys. Geosyst.* **5,** http://dx.doi.org/10.1029/2003gc000597 (2004).

Extended Data Table 1 | Major-element composition of silicate glass.

P = 1.5 GPa, T = 1400°C										
Run	**421**		**428**		**427**		**426**		**429**	
n	25	σ	20	σ	23	σ	19	σ	31	σ
SiO_2	56.19	0.28	57.69	0.25	59.63	0.80	57.93	0.01	48.14	0.26
Al_2O_3	20.50	0.14	20.40	0.11	20.21	0.11	19.60	0.09	18.17	0.16
CaO	11.48	0.08	13.02	0.09	10.97	0.07	10.48	0.16	9.39	0.08
MgO	6.66	0.06	6.53	0.06	6.50	0.11	6.22	0.08	5.61	0.05
FeO	3.15	0.07	1.21	0.04	0.56	0.03	0.50	0.23	16.36	0.13
S	0.11	0.01	0.18	0.01	0.34	0.02	6.11	0.24	0.24	0.02
Σ trace	0.81	0.02	0.90	0.02	0.78	0.04	0.30	0.03	0.65	0.05
Total	98.90		99.93		98.99		101.14		98.56	

P = 1.5 GPa, T = 1650°C								
Run	**461**		**462**		**477**		**464**	
n	43	σ	40	σ	31	σ	27	σ
SiO_2	53.28	0.84	58.38	0.22	58.51	0.80	58.60	0.31
Al_2O_3	21.64	0.62	20.32	0.12	19.00	0.26	19.17	0.23
CaO	12.02	0.08	10.78	0.09	9.89	0.12	9.15	0.08
MgO	8.13	0.29	7.01	0.13	5.99	0.10	6.20	0.06
FeO	1.98	0.11	0.61	0.09	0.51	0.20	0.48	0.08
S	0.42	0.04	1.39	0.08	5.93	0.12	7.18	0.12
Σ trace	0.79	0.03	0.75	0.01	0.44	0.01	0.40	0.01
Total	98.26		99.24		100.27		101.18	

P = 1.5 GPa, T = 1500°C								
Run	**1414**		**1415**		**1416**		**1417**	
n	26	σ	22	σ	26	σ	31	σ
SiO_2	48.86	0.34	50.66	0.34	41.12	0.43	39.28	0.36
Al_2O_3	16.58	0.16	13.87	0.16	15.95	0.16	15.00	0.17
CaO	15.14	0.09	13.16	0.07	14.91	0.14	14.12	0.16
MgO	15.99	0.12	14.11	0.07	15.51	0.12	15.05	0.17
FeO	0.61	0.11	0.41	0.06	7.51	0.28	11.59	0.5
S	0.79	0.03	6.98	0.08	0.25	0.13	0.24	0.24
Σ trace	2.01	0.04	1.55	0.04	2.28	0.03	2.16	0.10
Total	99.98		100.74		97.53		97.44	

Values are in weight per cent. σ calculated from error propagation. n is the number of measurements. Σ trace is the sum of trace elements measured using LA-ICP-MS.

Extended Data Table 2 | Major-element composition of sulfides.

P = 1.5 GPa, T = 1400°C										
Run	**421**		**428**		**427**		**426**		**429**	
n	21	σ	27	σ	23	σ	25	σ	23	σ
O	0.92	0.78	0.36	0.05	0.21	0.04	0.20	0.15	3.06	0.21
S	36.85	1.26	36.00	0.39	36.86	0.33	35.63	1.46	33.24	0.25
Fe	60.97	0.37	62.15	0.52	62.34	0.37	62.51	1.08	62.52	0.18
Ni	0.23	0.43	0.35	0.06	0.29	0.05	0.36	0.10	0.32	0.02
Sm	n.m.	n.m.	n.m.	n.m.	n.m.	n.m.	n.m.	n.m.	n.m.	n.m.
U	n.m.	n.m.	n.m.	n.m.	n.m.	n.m.	n.m.	n.m.	n.m.	n.m.
Σ trace	0.005	0.0005	0.008	0.001	0.040	0.004	0.556	0.139	0.004	0.002
Total	98.98		98.87		99.74		99.26		99.14	

P = 1.5 GPa, T = 1650°C								
Run	**461**		**462**		**477**		**464**	
n	22	σ	25	σ	21	σ	22	σ
O	0.37	0.20	0.21	0.15	0.21	0.12	0.16	0.08
S	36.68	0.02	35.55	0.78	32.92	1.40	33.82	0.53
Fe	61.66	0.32	62.90	0.74	64.45	1.29	62.94	0.64
Ni	0.37	0.33	0.33	0.09	0.25	0.07	0.14	0.02
Sm	n.m.	n.m.	n.m.	n.m.	0.028	0.004	0.032	0.009
U	n.m.	n.m.	n.m.	n.m.	0.099	0.007	0.116	0.022
Σ trace	0.019	0.002	0.105	0.009	0.225	0.016	0.206	0.073
Total	99.11		99.09		98.18		97.41	

P = 1.5 GPa, T = 1500°C								
Run	**1414**		**1415**		**1416**		**1417**	
n	26	σ	40	σ	35	σ	35	σ
O	0.24	0.18	0.51	0.32	1.98	0.77	3.18	0.83
S	33.89	2.63	32.18	2.06	35.46	0.79	33.40	0.85
Fe	63.37	2.10	64.05	2.08	60.50	0.29	61.26	1.37
Ni	1.09	0.51	0.85	0.25	1.16	0.03	1.13	0.05
Sm	n.m.	n.m.	0.071	0.011	n.m.	n.m.	n.m.	n.m.
U	n.m.	n.m.	0.328	0.049	n.m.	n.m.	n.m.	n.m.
Σ trace	0.100	0.011	0.380	0.048	0.014	0.002	0.015	0.00
Total	98.69		98.37		99.11		98.99	

Values are in weight per cent. σ calculated from error propagation. n.m., not measured. n is the number of measurements. Σ trace is the sum of trace elements measured using LA-ICP-MS.

Extended Data Table 3 | Trace-element concentration in silicates.

P = 1.5 GPa, T = 1400°C										
Run	**421**		**428**		**427**		**426**		**429**	
n	5	σ	5	σ	5	σ	5	σ	5	σ
Zr90	1226	29	1153	43	1171	49	206	55	956	72
La139	641	21	574	8	607	31	247	25	511	39
Ce140	4.0	0.1	4	0.1	3.7	0.4	2	0	3.4	0.4
Nd142	494	15	450	6	474	27	167	25	397	30
Sm152	796	25	728	9	775	39	304	30	645	50
Eu153	709	13	670	11	636	37	452	24	578	47
Yb174	1002	31	903	6	1009	42	590	25	799	57
Th232	1030	21	967	14	984	51	465	37	813	57
U238	961	21	929	22	893	43	117	4	782	52
Ni60	n.m.	n.m.	n.m.	n.m.	34	12	108	3	7	1

P = 1.5 GPa, T = 1650°C								
Run	**461**		**462**		**477**		**464**	
n	5	σ	5	σ	5	σ	5	σ
Zr90	1174	26	1191	19	413	4	311	8
La139	632	24	568	2	387	8	367	11
Ce140	4.7	0.4	3.8	0.2	3	0.1	2.5	0.1
Nd142	489	18	441	6	278	6	325	7
Sm152	780	30	715	7	477	7	435	6
Eu153	661	31	624	7	557	6	499	18
Yb174	985	29	1028	22	739	9	683	20
Th232	980	24	1030	17	712	12	640	16
U238	922	35	689	12	159	1	135	3
Ni60	n.m.	n.m.	20	11	9	8	4	0

P = 1.5 GPa, T = 1500°C								
Run	**1414**		**1415**		**1416**		**1417**	
n	5	σ	5	σ	5	σ	5	σ
Zr90	3048	52	2287	53	3455	35	3133	38
La139	1558	25	1190	29	1752	27	1746	20
Ce140	3.0	0.2	2.0	0.2	3.1	0.1	3.0	0.2
Nd142	1222	23	917	18	1393	18	1372	21
Sm152	2062	40	1583	32	2290	24	2231	40
Eu153	1642	31	1422	31	1985	28	1957	21
Yb174	2466	54	2312	53	2838	27	2580	29
Th232	2551	51	2454	59	2887	32	2636	51
U238	2439	49	932	27	2688	38	2606	45
Ni60	17	10	10	5	13	1	21	3

Values are in parts per million. *n* is the number of measurements. n.m., not measured.

Extended Data Table 4 | Trace-element concentration in sulfides.

P = 1.5 GPa, T = 1400°C										
Run	**421**		**428**		**427**		**426**		**429**	
n	5	σ	5	σ	5	σ	5	σ	5	σ
Zr90	0.5	0.0	1.2	0.2	6	1	1228	58	2.2	1.0
La139	4.1	0.4	10	1	47	7	573	12	2.8	1.7
Ce140	0.1	0.1	0.1	0.03	0.4	0.1	4	0	0.0	0.0
Nd142	3.2	0.5	8	1	38	3	472	16	2.1	1.2
Sm152	3.6	0.5	9	1	48	4	683	13	3.2	2.1
Eu153	19	2	47	8	94	11	140	1	5.9	2.5
Yb174	0.7	0.3	1.8	0.1	8	1	218	12	2.7	2.9
Th232	0.4	0.1	0.7	0.1	3.1	0.3	339	6	3.0	2.8
U238	11	1	19	1	101	6	1792	94	14	3
Ni60	2837	64	3596	138	3320	88	3764	159	3153	51

P = 1.5 GPa, T = 1650°C								
Run	**461**		**462**		**477**		**464**	
n	5	σ	5	σ	5	σ	5	σ
Zr90	3.5	0.4	77	3	909	66	840	194
La139	17	1	80	7	201	17	151	119
Ce140	0.16	0.03	0.7	0.1	2	0.2	1.8	0.9
Nd142	14	1	76	7	192	14	275	28
Sm152	18	2	110	8	300	18	327	31
Eu153	62	3	109	11	131	12	78	58
Yb174	4.8	0.4	43	3	179	4	142	82
Th232	2.5	0.3	26	3	184	15	156	121
U238	41	4	380	36	927	43	952	74
Ni60	3643	90	3130	133	2573	181	1538	103

P = 1.5 GPa, T = 1500°C								
Run	**1414**		**1415**		**1416**		**1417**	
n	5	σ	5	σ	5	σ	5	σ
Zr90	12	3	1639	223	2.8	0.4	9	4
La139	106	8	564	65	16	2	14	1
Ce140	0.2	0.1	1.3	0.2	0.04	0.01	0.06	0.02
Nd142	77	5	491	42	12	1	11	1
Sm152	100	7	719	42	14	1	15	2
Eu153	471	51	569	63	59	5	35	3
Yb174	16	2	225	54	3.9	0.2	8	5
Th232	7	2	315	31	3.1	0.3	8	2
U238	216	36	2958	196	44	2	53	4
Ni60	10728	381	8480	386	9234	149	11066	72

Values are in parts per million. *n* is the number of measurements.

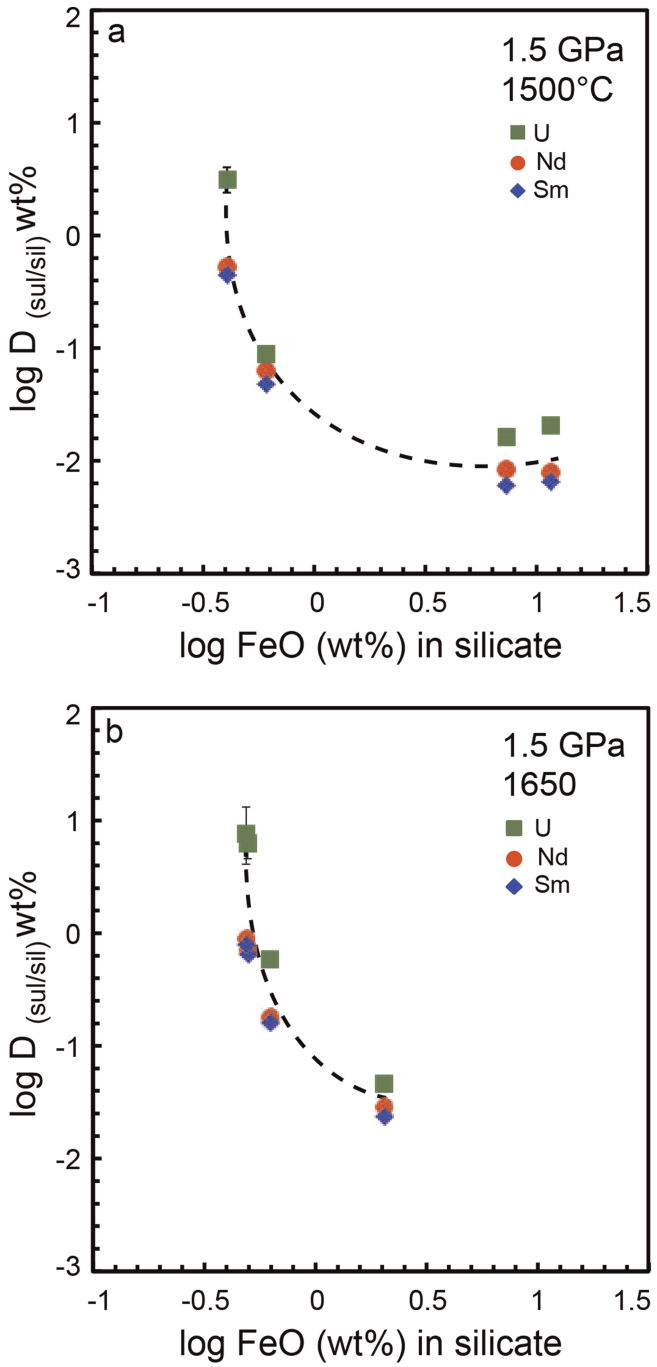

Extended Data Figure 1 | Partition coefficients for U, Nd and Sm with changing log[FeO] content in silicate melt (wt%). a, Results for *D* values of experiments performed at 1.5 GPa and 1,500 °C. **b**, *D* value results at 1.5 GPa and 1,650 °C.

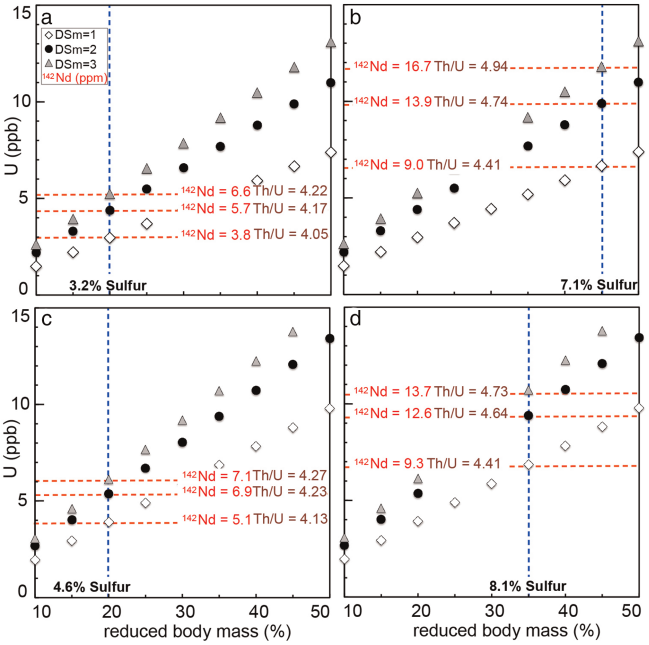

Extended Data Figure 2 | Core content of U (p.p.b.) and mantle ^{142}Nd anomaly (p.p.m.) at D_U/D_{Sm}=3. The effect on the Nd and U content using the same parameters (D_{Nd}/D_{Sm} at 1.4 and D_{Th}/D_U at 0.1) as in Fig. 2 but with a higher D_U/D_{Sm} ratio. **a** and **b** show the calculated effect of adding to Earth a reduced body of 20% of the Earth's mass or 45% of the Earth's mass, containing 0.15 mass fraction sulfide. **c** and **d** illustrate the same scenario except that the reduced body contains 0.22 mass fraction sulfide.

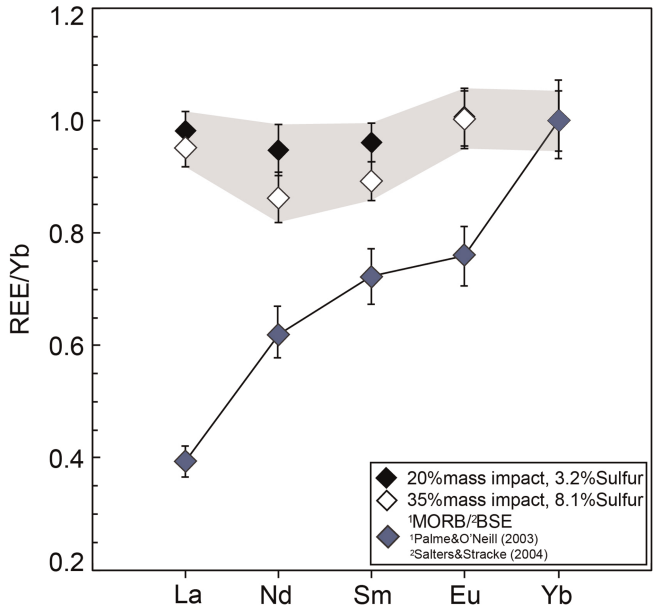

Extended Data Figure 3 | REE fractionation at 3.2% and 8.1% S in the core. The calculated REE pattern in the bulk silicate Earth (BSE) for the two extreme cases of Fig. 1a (3.2% S) and Extended Data Fig. 2d (8.1% S). Black diamonds represent REE concentrations relative to chondritic abundances and normalized to Yb = 1, at 3.2% S in the core (20% reduced mass impactor containing 0.15 mass fraction sulfide). White diamonds illustrate the REE fractionation at elevated S content (8.1% S in the core, 35% reduced mass impactor containing 0.22 mass fraction sulfide). We assumed D_{Sm} = [(Sm in sulfide)/(Sm in silicate)]=1 and D_i/D_{Sm} ratios for other elements from experiment 464. Both scenarios result in very small depletions of light REE relative to heavy REE in the BSE. The trend is broadly consistent with that seen in the depleted mid-ocean-ridge basalt (MORB)−mantle composition (blue diamonds) but much smaller. The effect on the REE pattern of the BSE would, as can be seen, be undetectable. Blue diamonds illustrate the measured ratio of depleted MORB mantle (from Salters and Stracke[31]) to the BSE (Palme and O'Neill[8], assuming chondritic abundances of refractory lithophile elements in the latter. Error bars are from propagated error calculation and correspond to 1 s.d.

heterogeneity might be intrinsic to the metastatic process. Indeed, a mouse model of small-cell lung cancer also shows evidence of polyclonal metastatic seeding[7]. Such seeding might be favoured when two or more distinct tumour subclones cooperate to promote their mutual growth and survival[8–10]. Furthermore, analyses of circulating tumour cells in breast cancer show that metastatic seeding is frequently mediated by small clusters of tumour cells containing multiple clones, rather than by single cells[11].

Taken together, the current studies might explain why, given the prevalence of circulating tumour cells in patients with solid tumours, successful metastasis is relatively rare — metastasis may be facilitated by seeding by cell clusters containing cooperating clones with distinct properties. If so, it is attractive to speculate that disseminated single cells could remain dormant until reawakened by interaction with a cooperative metastatic cell arriving at the same secondary site. Such a model has the potential to revise our conception of the properties of tumour-initiating cells, as well the metastatic niche, and may have implications for therapeutic strategies. For example, understanding the signalling pathways that mediate such clonal cooperativity may lead to effective therapies using drugs that target these pathways.

Future advances in understanding early events in metastatic seeding will require functional analyses to investigate molecular mechanisms. At present, however, the availability of suitable model systems for such studies is limited. Advances might come from the use of lineage tracing to follow metastasis in genetically engineered mice[12], alongside mathematical methods that assess clonal relationships from genomic data. The development of these and other experimental approaches will undoubtedly accelerate our understanding of the complexity of metastasis. ■

Michael M. Shen *is in the Departments of Medicine, of Genetics and Development, of Urology and of Systems Biology, and at the Herbert Irving Comprehensive Cancer Center, Columbia University Medical Center, New York, New York 10032, USA.*
e-mail: mshen@columbia.edu

1. Fidler, I. J. *Nature Rev. Cancer* **3,** 453–458 (2003).
2. Liu, W. *et al. Nature Med.* **15,** 559–565 (2009).
3. Sethi, N. & Kang, Y. *Nature Rev. Cancer* **11,** 735–748 (2011).
4. Gundem, G. *et al. Nature* **520,** 353–357 (2015).
5. Hong, M. K. H. *et al. Nature Commun.* http://dx.doi.org/10.1038/ncomms7605 (2015).
6. Burrell, R. A., McGranahan, N., Bartek, J. & Swanton, C. *Nature* **501,** 338–345 (2013).
7. McFadden, D. G. *et al. Cell* **156,** 1298–1311 (2014).
8. Calbo, J. *et al. Cancer Cell* **19,** 244–256 (2011).
9. Cleary, A. S., Leonard, T. L., Gestl, S. A. & Gunther, E. J. *Nature* **508,** 113–117 (2014).
10. Marusyk, A. *et al. Nature* **514,** 54–58 (2014).
11. Aceto, N. *et al. Cell* **158,** 1110–1122 (2014).
12. Aytes, A. *et al. Proc. Natl Acad. Sci. USA* **110,** E3506–E3515 (2013).

This article was published online on 1 April 2015.

PLANETARY SCIENCE

A new recipe for Earth formation

Experimental results suggest that if Earth initially grew by the accumulation of highly chemically reduced material, its core could contain enough uranium to drive the planet's magnetic field throughout Earth's history. SEE LETTER P.337

RICHARD W. CARLSON

Determining Earth's bulk composition is difficult because so little of the planet is directly accessible. As a result, most estimates derive from a comparison of Earth rocks with the planet's probable building blocks — the asteroidal bodies sampled by meteorites. New views about the mechanism of planet formation, and their consequences for estimating Earth's composition, are, surprisingly, being driven by observations of planetary systems around stars other than the Sun. On page 337 of this issue, Wohlers and Wood[1] report experiments that explore the consequences of one of these views — that the building blocks of Earth systematically changed composition during its growth. Their results lead to the intriguing conclusion that if Earth formation started with highly chemically reduced building blocks, the planet's metallic core might contain enough uranium to power the convection that creates, and has maintained, Earth's magnetic field for more than 3 billion years.

Most models of planet formation predict that planets grow by the accumulation of smaller bodies known as planetesimals, measuring about 10–100 kilometres in diameter[2]. Planetesimals that form far from the central star are cold enough to include ices, whereas those formed in the hotter region close to the star are largely composed of mixtures of silicate and iron metal. This simple model fits well with the observation of our Solar System's 'snow line', which separates rocky Mars from the giant gaseous outer planets. This implies that planets grow mostly from material that is formed at similar distances from the Sun, and that planets stay in the positions where they are made.

This comforting view of planetary orbital stability was lost with the detection of 'hot Jupiters'[3] — large gaseous planets in orbit close to their stars. These close-in giant planets may have formed far from their suns, as did Jupiter, but then migrated inwards, probably during the period of planet growth. Building on these observations, a theoretical model for planet formation in the Solar System suggests that Jupiter and Saturn may have migrated inwards until gravitational interaction between the two caused them to retreat outwards to their current positions[4].

Because these giant planets are the gravitational heavyweights of the outer Solar System, their migration during or after the period of planet growth would have scattered smaller planetesimals from their path. This could have resulted in material being cleared from the area where Mars now exists, explaining the planet's small size. If this migration occurred while Earth was forming, the materials from which Earth grew would have changed from those that formed close to the Sun, near Earth's current orbit, to those that formed far from the Sun and were forced into the inner Solar System as they fled in front of inward-migrating Jupiter.

Wohlers and Wood's experiments explore the effects of Earth growing first from the accumulation of highly reduced material, in which most iron is present as metal or sulfide, followed by the accumulation of more-oxidized material, in which a good fraction of the iron is present as iron oxide incorporated into silicate minerals. Within the meteorites delivered to Earth, both highly reduced and highly oxidized varieties exist, so this compositional variation is not just hypothetical. In addition, the discovery of high concentrations of sulfur on the surface of Mercury[5] (Fig. 1) suggests that Mercury is dominated by reduced material, because sulfur is much more volatile when oxidized than when it is reduced. Given Mercury's proximity to the Sun, one might expect it to have formed hot, in which case it should be depleted in sulfur unless it formed preferentially from reduced material.

At present, Earth is quite oxidized. Under these conditions, many elements, including uranium (U), thorium (Th) and the rare-earth elements — those with atomic numbers 57 to 71, such as neodymium (Nd) and samarium (Sm) — are not at all soluble in iron metal or iron sulfide. In this case, Earth's total inventory of U, Th and the rare-earth elements should be

present in the silicate portion of Earth (the crust and mantle), with only insignificant quantities in the planet's iron-metal core. Wohlers and Wood's experiments explored the partitioning of these elements between iron metal, iron sulfide and silicates at different oxidation states. Under very reducing conditions, such as those that might have been involved in Mercury's formation, their results show that U and the lighter of the rare-earth elements, but not Th, become soluble in iron sulfide, which would have joined the iron metal in Earth's core.

The energy source that drives the generation of Earth's magnetic field in the core has long been a topic of discussion, as has the suggestion that one such energy source could be a moderate concentration of uranium or potassium in the core. However, before Wohlers and Wood's experiments, there was only limited (and controversial) experimental evidence that either uranium or potassium can be incorporated in iron metal at the high temperatures and pressures of core formation.

Because U, Th and most of the rare-earth elements condense at very high temperatures from a gas of solar composition, Earth should in principle have accumulated all of these elements in relative abundances similar to those of the Sun — so Earth's bulk abundance ratios of Th to U (Th/U) and Sm to Nd (Sm/Nd) should be the same as the Sun's. But if the core contains a significant amount of U and Nd, as Wohlers and Wood's results suggest, the silicate Earth should be left with higher Th/U and Sm/Nd ratios than those of the Sun. Estimates of the silicate Earth's Th/U ratio are indeed higher than the solar value, but not by enough to make a convincing case for such a selective incorporation of U into the core.

A more stringent test of whether U was incorporated into the core through the mechanism proposed by Wohlers and Wood might be provided by the isotopic composition of Nd in the silicate Earth. This composition is modified by the radioactive decay of two isotopes of Sm — ^{147}Sm (half-life of 106 billion years) and ^{146}Sm (half-life of 103 million years). The average Nd isotopic composition in the silicate Earth was thought to be similar to that of the Sun, with small deviations caused by the chemical separation of a crust with a low Sm/Nd ratio that left the mantle with an elevated Sm/Nd ratio. This assumption began to be questioned when high-precision Nd-isotope measurements in 2005 showed that both crustal and mantle rocks on Earth have a higher ^{142}Nd/^{144}Nd ratio than the Sun[6] (note that ^{142}Nd is the product of the decay of ^{146}Sm).

Given the short half-life of ^{146}Sm, the elevated ^{142}Nd/^{144}Nd ratio of the silicate Earth reflects a higher than solar Sm/Nd ratio that must have been present in the silicate Earth since shortly after its formation. Earth's core formed within tens of millions of years after the formation of the Solar System, so preferential incorporation of Nd into the core, as suggested by Wohlers and Wood's results, would leave the whole silicate Earth with an elevated Sm/Nd ratio that could explain its high ^{142}Nd/^{144}Nd ratio.

To simultaneously satisfy the Th/U and ^{142}Nd/^{144}Nd ratios of the silicate Earth, Wohlers and Wood propose a balance between the amounts of reduced and oxidized materials added to the planet. Although possible, this carefully balanced ratio must also satisfy other potential geochemical consequences of involving highly reduced materials in Earth-formation models — not least, how Earth ended up in its present oxidized state, which it has apparently retained for more than 3 billion years. ■

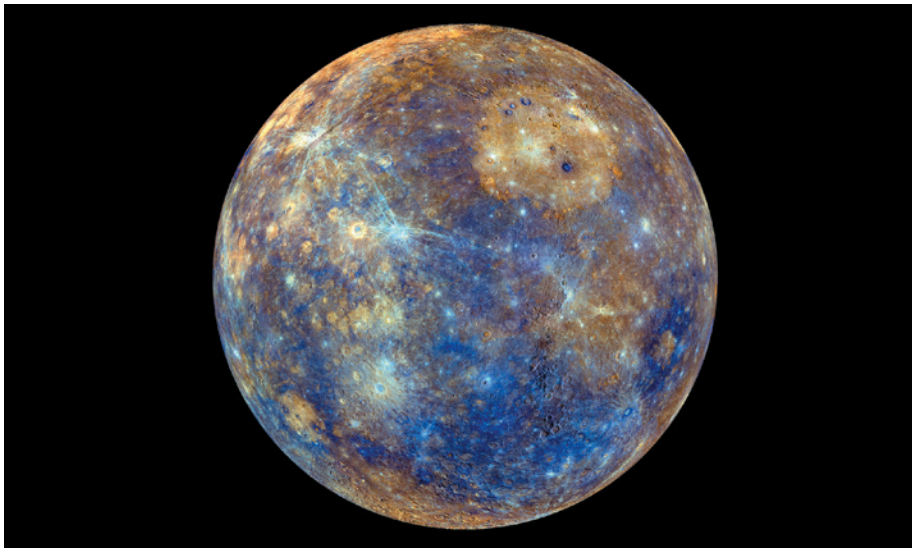

NASA/JOHNS HOPKINS UNIV. APPLIED PHYSICS LAB./CARNEGIE INST. WASHINGTON

Figure 1 | Mercury's surface. The image is a false-colour mosaic of images of Mercury obtained by NASA's MESSENGER spacecraft. Parts of the planet's surface have atomic ratios of sulfur to silicon that are more than 0.14, compared with values of 0.001 in Earth's mantle[5]. These ratios probably reflect chemically reduced conditions in which sulfur is predominantly contained in iron sulfide, unlike on Earth's surface, where sulfur is mostly in the form of oxidized sulfate. Wohlers and Wood's results[1] indicate that, if Earth's growth initially involved the accumulation of a reduced, Mercury-like body, significant amounts of Earth's uranium may be present in the planet's core.

Richard W. Carlson *is in the Department of Terrestrial Magnetism, Carnegie Institution for Science, Washington DC 20015, USA.*
e-mail: rcarlson@carnegiescience.edu

1. Wohlers, A. & Wood, B. J. *Nature* **520,** 337–340 (2015).
2. Chambers, J. E. *Earth Planet. Sci. Lett.* **223,** 241–252 (2004).
3. Marcy, G. W. & Butler, R. P. *Astrophys. J. Lett.* **464,** L147 (1996).
4. Walsh, K. J., Morbidelli, A., Raymond, S. N., O'Brien, D. P. & Mandell, A. M. *Nature* **475,** 206–209 (2011).
5. Weider, S. Z. *et al. Earth Planet. Sci. Lett.* **416,** 109–120 (2015).
6. Boyet, M. & Carlson, R. W. *Science* **309,** 576–581 (2005).

CANCER

An extravascular route for tumour cells

Molecular tracing of populations of breast-cancer cells in a primary tumour in mice reveals that two proteins, Serpine2 and Slpi, enable tumour cells to form vascular-like networks, facilitating perfusion and metastasis. SEE LETTER P.358

MARY J. C. HENDRIX

Cancer deaths result primarily from metastases, which comprise mixed populations of tumour cells and which are often resistant to conventional therapies. Metastasis is a complex, multistep process, in which cells escape from the primary tumour through the vasculature, move from the vascular system into the target organ, and then form secondary tumours[1]. Efforts to study the metastatic properties of different tumour cells that are involved in each aspect of this process have been challenged by inadequate tools — until now. In this issue, Wagenblast *et al.*[2] (page 358) deploy an innovative 'molecular-barcoding'